# Hybrid thermochemical cycles for low-grade heat storage and conversion into cold and / or power

Alexis Godefroy, Maxime Perier-Muzet, Pierre Neveu, Nathalie Mazet

# Hybrid thermochemical cycles for low-grade heat storage and conversion into cold and / or power

***Alexis Godefroy[a,b], Maxime Périer-Muzet[a,b], Pierre Neveu[a,b] and Nathalie Mazet[a]***

*[a] CNRS-PROMES Laboratoire PROcédés, Matériaux et Energie Solaire, 66100 Perpignan, France, contact@promes.cnrs.fr*
*[b] UPVD Université de Perpignan Via Domitia, 66100 Perpignan, France, Corresponding author: alexis.godefroy@promes.cnrs.fr*

**Abstract:**

In order to recover low grade heat (available at temperatures under 250 °C) provided for instance by an industrial plant or solar energy, innovative thermodynamic cycles are investigated. These cycles are based on the hybridization of a solid/gas chemical sorption cycle (thermochemical cycle) with a power cycle (Organic Rankine Cycle (ORC)), they enable converting a low grade heat input into cold and / or power while providing an intrinsic energy storage feature. Four hybrid configurations are considered, a thermodynamic analysis allows comparing their performances with those of existing ORC through several criteria: energy and exergy efficiencies, specific exergy output and power production ratio. For each of the five systems, potential applications, advantages and weaknesses are summarized.

**Keywords**:
Low grade heat recovery, Cogeneration of power and refrigeration, Thermochemical energy storage, Thermodynamic analysis, Organic Rankine Cycle.

## 1. Introduction

As regards both energy demand and resources, the management of variability is a decisive issue; this topic covers variability in energy form (which can be addressed through developing multi-purpose systems) and time-variability (which can be addressed through integrating energy storage systems).

In this context, an interesting option consists in pooling devices of two thermodynamic cycles, in order to combine their functionalities and build a so-called "hybrid" system. This may lead to a substantial improvement in flexibility and efficiency. To that end, the most relevant cycles are:

1. Three-temperatures cycles involving a liquid / gas sorption process (absorption). Using evaporation / condensation of a vapor flow and its absorption / desorption in a liquid solution (typically $H_2O$ / LiBr), they take advantage of the related thermal effects (either exo- or endothermal effect, according to the component). Since the liquid solution flows between vapor desorber and absorber, a continuous cold (at the evaporator) or heat (at the absorber) production is achieved. These systems are characterized by quite good COP (from 0.7 to 1).
2. Three-temperatures cycles involving a solid / gas sorption process (thermochemical). Although the operating mode is similar to liquid / gas absorption cycles, it is based on a reversible solid / gas chemical reaction (exothermal synthesis / endothermal decomposition). Hence, these cycles are discontinuous: an intrinsic storage feature is thereby provided, with

high energy densities [1]. Moreover, they can operate in a wide range of operating conditions (T, P) depending on the reactive pair [2].

3. Two-temperatures power cycles: Organic Rankine Cycles (ORC) provide an efficient mechanical energy production from a low grade heat source. Adjusting the working fluid and components allows optimizing the mechanical work production.

Both of these three cycles involve a working fluid undergoing state changes in vapor generators and absorbers (evaporator / condenser, desorber / absorber, sorption reactors). Consequently, coupling and hybridizing them will consist in coupling these common components.

Considering the three-temperatures liquid / gas absorption cycle and the two-temperatures power cycle, several hybrid configurations were proposed: firstly, Kalina cycle (power cycle developed from the late 1970s) involves a binary mixture as working fluid (typically $NH_3$ / $H_2O$) in order to decrease thermodynamic irreversibility caused by temperature mismatch during heat transfer. With a hot source temperature of 399 °C, its energy efficiency ranges from 0.15 to 0.20 and exergy efficiency is approximately 0.52 [3]. Later, Goswami et al. [4-5] proposed an absorption power cycle providing additional cold production. For this system, providing cold at -10 °C using a 140 °C hot source temperature, energy efficiency ranges from 0.17 to 0.24 while exergy efficiency ranges from 0.49 to 0.65. Concerning ORC, Kalina and Goswami cycles, a review was proposed by Karimi et al. [6].

Considering thermochemical cycle and two-temperatures power cycle, very few hybrid configurations have been studied despite the interesting storage feature of thermochemical cycles. In this area, the main investigations have been carried out on resorption cycles:

- For power production only, Jiang et al. [7] obtained energy and exergy efficiencies ranging respectively from 0.07 to 0.12 and 0.40 to 0.74, with a hot source temperature below 110 °C.
- For power & cold cogeneration, one of the first resorption cycles was proposed by Wang et al. [8], and later improved by Lu et al. [9]. Providing cold at 10 °C with a hot source temperature of 110 °C, its COP ranges from 0.83 to 0.93 while exergy efficiency ranges from 0.32 to 0.41. The theoretical and experimental works of Jiang et al. [10-11] lead to energy and exergy efficiencies in the ranges [0.29; 0.42] and [0.12; 0.16] respectively (hot source between 120 and 170 °C, cold production at 10 °C).

Finally, an innovative hybrid cycle based on solid / gas chemical sorption was proposed by Bao et al. [12] for the cogeneration of power and cold. COP and exergy efficiencies are respectively in the ranges [0.34; 0.57] and [0.20; 0.62] (hot source between 85 and 255 °C, cold production at -10 °C).

In this paper, innovative hybrid thermochemical cycles for cold and / or power production are investigated using a new methodology, which underlines the sensitivity of the performances to a wide variety of reactive salts. Firstly, the working principle of hybrid thermochemical cycles is presented (components and thermodynamic path), which leads to identify four operating modes for these cycles; then, the framework of the thermodynamic study (assumptions, methodology, performance criteria) is depicted. The following section gathers performance results of both hybrid cycles and ORC, for hot source temperatures under 250 °C. Finally, conclusions are drawn on advantages, weaknesses and possible applications of the five systems in the field of low grade heat recovery.

# 2. Hybrid cycles for cold and / or power production

## 2.1. Working principle: general overview

Hybridizing a thermochemical refrigeration cycle with a power cycle leads to the general scheme of Fig. 1. Since it uses a solid sorbent, this system is intrinsically discontinuous: this characteristic provides the **storage function** of the cycle. Its operation is divided into two steps:

- The charging step (step 1) occurs when a hot source is available (high pressure levels).
- The discharging step (step 2) is performed when a useful effect is needed (low pressure levels).

Each of these two operating steps comprises two main components:

- A vapor generator, where an endothermal process (decomposition reaction of a solid sorbent or evaporation of the liquid working fluid) takes place.
- A vapor absorber, where an exothermal process (synthesis reaction of a solid sorbent or condensation of the gaseous working fluid) takes place.

Regarding **heat flows**, a heat input ($Q_{in}$) is required for the high pressure endothermal process (charging step), while a **cold production function** ($Q_{cold}$) may be provided by the low pressure endothermal process (discharging step). Furthermore, heat is rejected at ambient ($Q_{amb}$) and mid-temperature ($Q_m$) by respectively, the high and low pressure exothermal processes.

Regarding **mass flows**, in each step, an expander is located between the vapor generator and absorber to take advantage of the reactive vapor flow leaving the vapor generator: it can be either actuated (leading to a non-isobaric step) or bypassed (leading to an isobaric step) as illustrated by the valves on Fig. 1: this provides the **power production function** ($W_1$ and $W_2$) of the cycle.

Based on Fig. 1, four hybrid cycles (operating **modes**) are thus considered:

- Separated power & cold mode: the expander is actuated in charging step only (isobaric discharging step, $W_2 = 0$). Therefore, cold and power productions are time-shifted: power is generated in charging step while cold is produced in discharging step.
- Simultaneous power & cold mode: the expander is actuated in discharging step only (isobaric charging step, $W_1 = 0$). Therefore, both cold and power are produced in discharging step.
- Combined power & cold mode: the expander is actuated in both of the two steps of operation (non-isobaric steps, $W_1 \neq 0$ and $W_2 \neq 0$). This enables increasing the total power output.
- Power mode with auto-thermal discharging step: the expander is actuated in discharging step only (isobaric charging step, $W_1 = 0$). Moreover, in this step, the heat $Q_m$ (from the vapor absorber) is transferred to the vapor generator. Thus, the vapor generator pressure and temperature increase: cold production is removed, in favor of an increased power production.

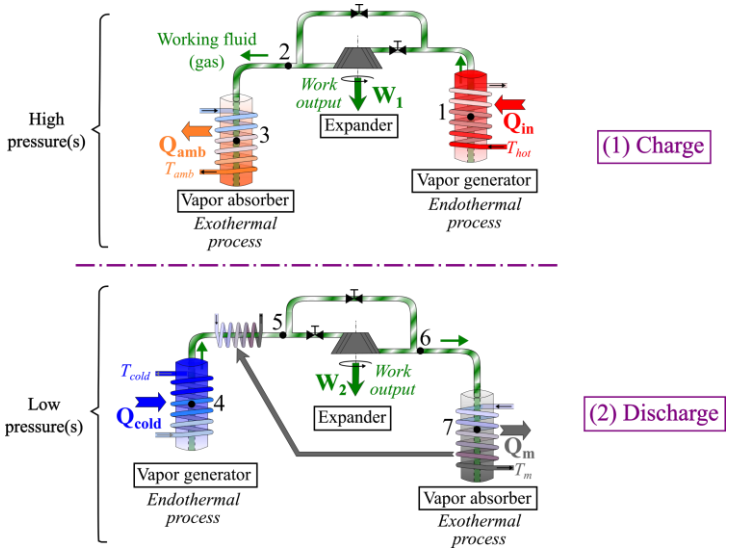


*Figure 1. Working principle of hybrid thermochemical cycles: components, mass and energy flows in each step of operation (Charge / Discharge).*

## 2.2. Thermodynamic path

In connection with Fig. 1 (working principle with components), Fig. 2 shows the thermodynamic cycle followed by the working fluid, ammonia. This is the Clausius-Clapeyron diagram ($ln(P/P^0)$ as a function of $-1/T$), well known for thermochemical systems. As highlighted by this diagram, hybrid thermochemical cycle operation is based on the existence of two thermodynamic equilibrium lines:

- The High Temperature equilibrium is associated to High Temperature Material (HTM), which is a solid reactive salt. This is a chemical reaction equilibrium.

- The Low Temperature equilibrium relates to Low Temperature Material (LTM), which is:
  - Either ammonia. In this case, named **single sorption** cycle, the Low Temperature equilibrium is a liquid / vapor phase change equilibrium.
  - Or a solid reactive salt. In this case, named **resorption** cycle, the Low Temperature equilibrium is a chemical reaction equilibrium.

Based on Fig. 2, the operation of the hybrid cycle is illustrated for the combined power & cold mode:

- During the charging step, heat supply ($Q_{in}$) drives the endothermal desorption of ammonia, which is released close to the HTM equilibrium conditions (point 1). The reactive fluid is then expanded (between points 1 and 2) and finally condensed or absorbed (point 3).
- During the discharging step, the endothermal evaporation or desorption of ammonia at a lower pressure (point 4) provides the cooling effect ($Q_{cold}$); ammonia vapor is superheated (between points 4 and 5), then expanded (between points 5 and 6) and finally absorbed (point 7).

More details on the operation of thermochemical cycles can be found in [13] and [14]. Note that ammonia liquid-vapor equilibrium is modelled by (1), while chemical reaction equilibrium is modelled by (2). Those equations are represented by straight lines on Fig. 2.

$$ln\left(\frac{P}{P^0}\right) = -\frac{L_{vap}}{R.T} + \frac{\Delta S_{vap}}{R} \quad (1)$$

$$ln\left(\frac{P}{P^0}\right) = -\frac{\Delta_r H^0}{R.T} + \frac{\Delta_r S^0}{R} \quad (2)$$

The definition of HTM is a decisive factor for the hot source temperature; moreover, depending on whether charging and discharging steps are isobaric or not, the three cogeneration modes (separated, simultaneous and combined power & cold modes) clearly arise on Fig. 2.

In power mode with auto-thermal discharging step, exothermal synthesis heat $Q_m$ (released at point 7) is used to achieve endothermal vapor generation (point 4) upstream of the expander in discharging step. Therefore, pressure $P_{dec,L}$ (or $P_{evap}$, according to the nature of the LTM) increases and cold production is replaced by an increased power production.

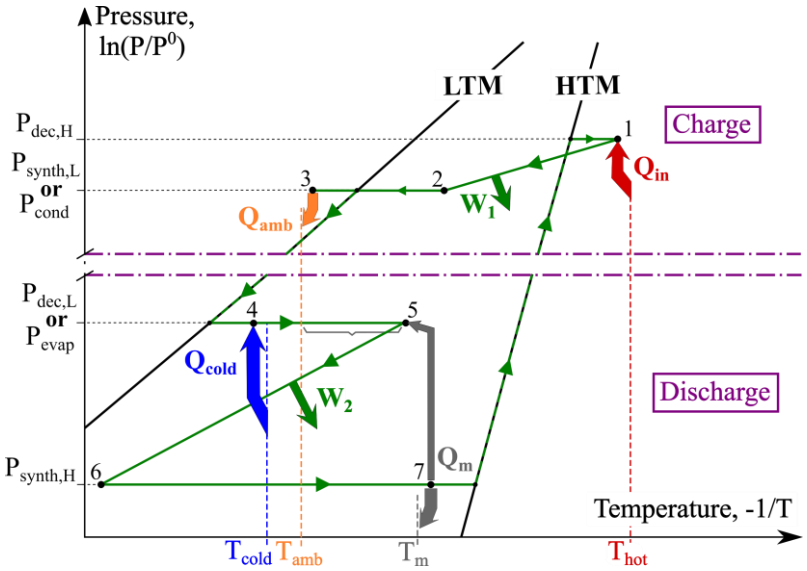


*Figure 2. Thermodynamic path followed by the working fluid of a hybrid thermochemical cycle: Clausius-Clapeyron diagram.*

# 3. Thermodynamic study

## 3.1. Operating conditions and main assumptions

The framework of the thermodynamic study is defined by the operating temperatures $T_{cold} = 0$ °C and $T_{amb} = 20$ °C; $T_{hot,max} = 250$ °C is set as the maximal hot source temperature since a focus is made on low grade heat sources. Moreover, the following thermodynamic assumptions are used:

- An isentropic efficiency $\eta_{is} = 0.8$ is set for expanders.
- The temperature pinch for (liquid / liquid) or (liquid / vapor) heat exchange is $\Delta T_{HX1} = 5$ K.
- The temperature pinch for (vapor / vapor) heat exchange is $\Delta T_{HX2} = 10$ K.
- The temperature deviation from thermodynamic equilibrium which is required for a chemical reaction to proceed is $\Delta T_{r\text{-}eq} = 20$ K.
- Reference temperature for exergy calculations is chosen as $T^0 = T_{amb} = 20$ °C.
- The pressure drops are neglected.
- There are no heat exchanges between components and the surroundings.

Beside, several technological boundary values are set:

- Working fluid pressure is bounded by $P_{min} = 0.1$ bar and $P_{max} = 30$ bar, for the sake of technical feasibility with acceptable costs.
- A minimal vapor quality $x_{min} = 0.8$ is required at the outlet of the expander.
- A maximal volumetric ratio $R_{v,max} = 10$ is assumed for expanders, to comply with their nominal operating range (scroll expanders are particularly targeted, as they are suitable for small facilities). To give an example, $R_v$ is defined as $R_v = v_6/v_5$ in discharging step on Fig. 2. Several expansion stages (number of expansion devices) are added to comply with this constraint.

Finally, this study is restricted to ammonia-salt reactive pairs in the thermochemical reactor. Thus, the working fluid of the whole hybrid thermochemical cycle is ammonia.

## 3.2. Methodology

All calculation processes described hereafter have been carried out with EES software [15].

### 3.2.1. Iterative algorithm: screening over the panel of reactive salts

This thermodynamic study is based on energy calculations. All extensive quantities related to each cycle ($Q_{in}$, $Q_{cold}$, masses, volumes, …) are computed for a given electrical production ($W = 1$ kWh). Specific values are then reported to the cycled mass of working fluid.

This thermodynamic study is aimed at exploring the potential of hybrid thermochemical cycles presented in §*2.* for different solid reactive salts, and to retrieve the most promising ones. A database containing thermochemical quantities (reaction enthalpy $\Delta_r H^0$ and reaction entropy $\Delta_r S^0$) for 103 reactive ammonia salts is used. The content of this database comes from values collected and computed by Touzain [16] and CNRS-PROMES knowledge. Among the gathered salts are mainly metallic chlorides, bromides and iodides, for instance: $CaCl_2$, $MnCl_2$, $FeBr_2$, $SrI_2$, …

The methodology of this study is divided into two main steps:

- Firstly, the LT equilibrium is set, being either a chemical reaction equilibrium (for resorption cycles), or an ammonia liquid – vapor equilibrium (for single sorption cycles).
- Secondly, for each one of the 103 reactive salts, its data $(\Delta_r H^0, \Delta_r S^0)$ are used to define the HT equilibrium, and the thermodynamic path (i.e. pressure, temperature, specific enthalpy and entropy at each key point of the cycle) is computed.

Note that, in the case of resorption cycles, a LTM has to be chosen in the first step. $BaCl_2$ (8/0) is chosen as the LTM for all resorption cycles in the next sections, since it enables cold production at

$T_{cold}$ with a decomposition reaction pressure ($P_{dec,L} = P_4$ on Fig. 2) at 0.09 bar, which is considered as acceptable despite the boundary value $P_{min} = 0.1$ bar.

Finally, a similar methodology was applied to realize a thermodynamic analysis of an ORC, considering 15 organic fluids (isobutene, n-pentane, R124, R134a, …).

### 3.2.2. Definition of relevant performance criteria

The LT and HT thermodynamic equilibria being known, and given that $W = 1$ kWh, the following quantities are computed at each iteration:

- Hot source temperature, $T_{hot}$ (depending on the HTM and temperature pinches).
- Volumetric expansion ratio(s), $R_v$ ($R_{v,1}$, $R_{v,2}$, … if there are several expansion stages).
- Heat consumption, $Q_{in}$.
- Cooling effect, $Q_{cold}$.

Note that a residual cold production $Q_{cold}$ may be observed in power mode with auto-thermal step (due to the cold outlet of the expander in discharging step): even if this is not the prioritized useful effect of this operating mode, it enables improving the cycle performances.

In order to pick out the most relevant reactive salts, 4 performance criteria are defined and computed for each HTM:

- Energy efficiency,

$$\eta_I = \frac{W + Q_{cold}}{Q_{in}} \tag{3}$$

- Exergy efficiency,

$$\eta_{ex} = \frac{W + Ex_{cold}}{Ex_{in}} \tag{4}$$

- Specific exergy output,

$$w + ex_{cold} = \frac{W + Ex_{cold}}{m_{wf}} \tag{5}$$

- Power production ratio,

$$\tau_w = \frac{W}{W + Q_{cold}} \tag{6}$$

, with $$Ex_{in} = Q_{in}.\left(1 - \frac{T^0}{T_{hot}}\right) \tag{7}$$

and $$Ex_{cold} = Q_{cold}.\left(\frac{T^0}{T_{cold}} - 1\right) \tag{8}$$

These performance criteria were chosen because they seemed to be the most relevant: without being redundant, they provide enough information to give a fair comparison between the cogeneration and power cycles presented in this study. Indeed:

- The energy efficiency $\eta_I$, defined in (3), is the ratio of useful energy to input energy. This is a cogeneration efficiency, which is suitable for comparison with other cogeneration cycles working under the same temperatures ($T_{cold}$, $T_{amb}$, $T_{hot}$).

- The exergy efficiency $\eta_{ex}$ defined by (4), which is the ratio of useful exergy to input exergy, accounts for the fact that mechanical work and heat do not have the same "quality", through the Carnot weighting factors related to $T_{hot}$ (according to (7)) and $T_{cold}$ (according to (8)).
- Specific exergy output $w+ex_{cold}$, as defined by (5), should be read alongside the two previous criteria, since it provides a quantitative assessment of both useful effects: respectively work generation and useful exergy are reported to mass unit of the working fluid.
- Finally, power production ratio $\tau_w$, defined in (6), gives the missing information to determine specific work output $w$ (see (9)). It should be read alongside $\eta_I$, whose order of magnitude greatly depends on the useful effects (cold and / or power).

$$w = \frac{\eta_I . \tau_w . (w + ex_{cold})}{\eta_{ex} . \left(1 - \frac{T^0}{T_{hot}}\right)} \quad (9)$$

Once the computations have been realized for all reactive salts, a first selection is made: thermodynamic cycles that cannot meet technological boundary values $R_{v,max}$, $x_{min}$, $P_{min}$, $P_{max}$ or $T_{hot,max}$ are excluded. The remaining salts are ranked according to each of the previous 4 criteria and, for each of these criteria, only the 10 best salts are retained. At the end of this process, about 15 to 30 solid salts are selected for each cycle configuration (see §4.).

Finally, a slightly different selection process was used for ORC: for each of the hot source temperatures obtained in the case of hybrid thermochemical cycles, the organic fluids having the best performances (over the criteria $\eta_I$, $\eta_{ex}$ and $w$) were retrieved.

As mentioned in §3.1., several expansion stages have to be implemented in some cases in order to fulfill the boundary value $R_{v,max}$. Only slight differences were observed between the performances of one- to three-expansion cycles. Consequently, only the configurations with the highest number of expansion stages (leading to the best exergy efficiencies) were retrieved in §4.

# 4. Results and discussions

Fig. 3 gathers the results for hybrid thermochemical cycles (4 operating modes) and ORC: for each system, the performance criteria of §3.2.2. are displayed as a function of hot source temperature $T_{hot}$.

On these plots, vertical black lines delimit three areas corresponding to the following hot source temperature ranges: [100; 150 °C], [150; 200 °C] and [200; 250 °C].

Concerning the required hot source temperatures:

- Power mode with auto-thermal step (red triangles) operates at $T_{hot} > 81$ °C.
- Simultaneous power & cold mode (green squares) operates at $T_{hot} > 107$ °C.
- Separated (blue triangles) and combined (pink circles) modes work at $T_{hot} > 138$ °C.
- Finally, ORC (black circles) can operate over the whole temperature range [81; 250 °C].

These differences can be explained using Fig. 2:

- Pressure $P_{dec,H}$ is higher in separated and combined modes ($W_1 \neq 0$), thus temperature $T_1$ (and, as a consequence, $T_{hot}$) is higher.
- The constraint $W_1 \neq 0$ does not apply in simultaneous power & cold mode, which reduces the minimal required hot source temperature. However, because of the constraint over $P_6$, all HTMs are not usable to achieve both cold and power production.

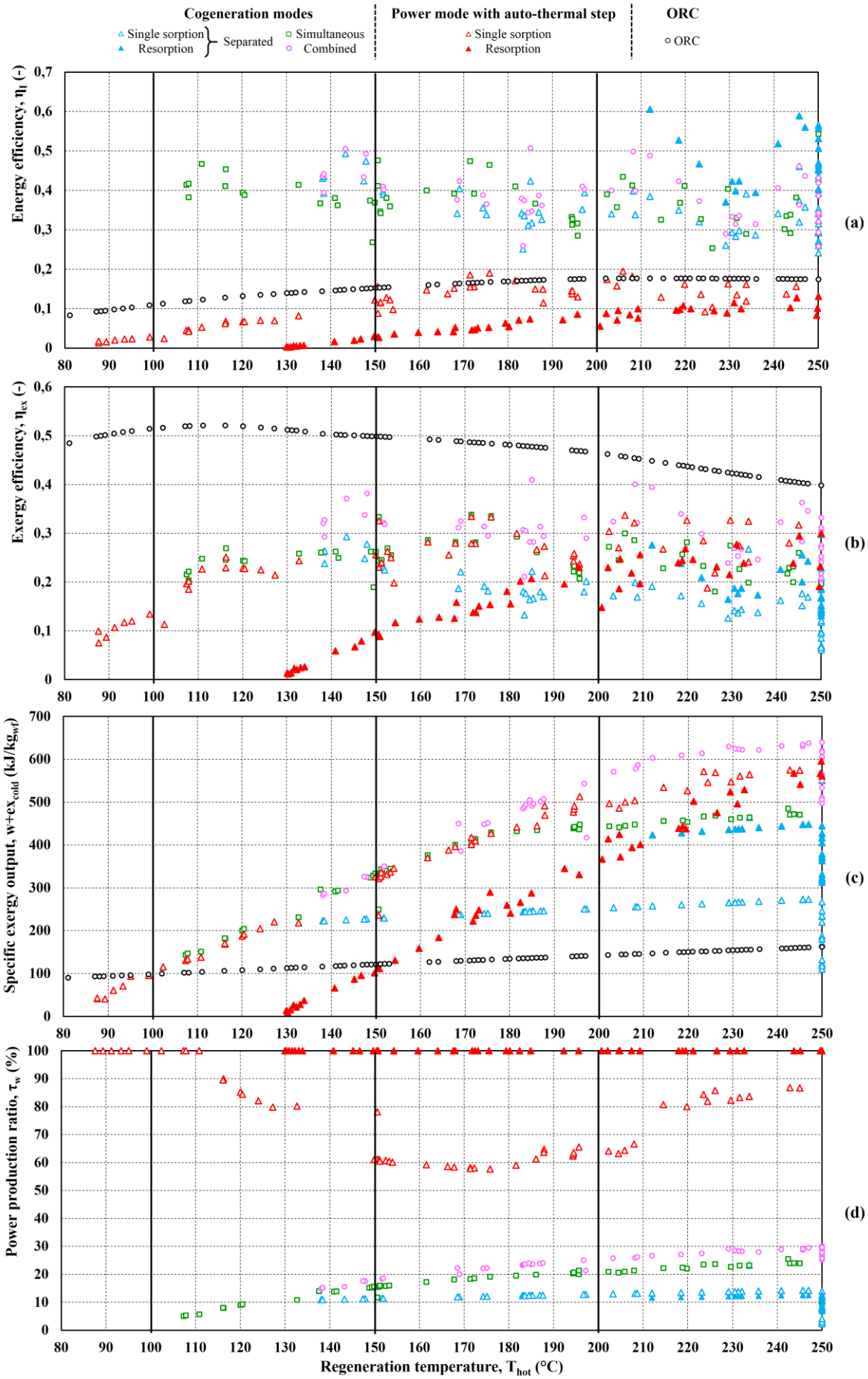


*Figure 3. Performance results of the 5 cycles: hybrid thermochemical cycles (4 operating modes) and ORC. Energy (a) and exergy (b) efficiency, specific exergy output (c) and power production ratio (d).*

- In the case of power mode with auto-thermal step, more HTMs can be used, which extends the minimal regeneration temperature.

Note that for a given operating mode, resorption cycles (filled triangles) require higher hot source temperatures than single sorption cycles to operate:

- In power mode with auto-thermal step, the minimal usable regeneration temperature is $T_{hot} =$ 130 °C in resorption case, against 81 °C for single sorption case.
- In separated power & cold mode, the minimal usable regeneration temperature is $T_{hot} = 212$ °C in resorption case, against 138 °C for single sorption case.

This difference is caused by the closeness of LT and HT equilibrium lines, which makes resorption cycle unfeasible for a lot of HTMs.

Power production ratio $\tau_w$ (Fig. 3d) supports the following analyses, especially about $\eta_I$ and $w+ex_{cold}$.

As regards energy efficiencies:

- All cogeneration cycles (separated, simultaneous and combined modes) show good performances: $\eta_I$ ranges from 0.24 to 0.61, against 0.08 to 0.18 for ORC and 0.01 to 0.20 for power cycle with auto-thermal step. These differences originate in different proportions of power and cold in useful effects: $\tau_w$ ranges from 2 to 30 % for cogeneration cycles, against 58 to 100 % for power mode with auto-thermal step and ORC. A higher proportion of cold production is always beneficial to energy efficiency, but a cooling effect is not as valuable as a power output due to the low related Carnot factor (see the exergy efficiency analysis).
- The best values are reached with resorption cycles (filled blue triangles), because their cold production is higher (it originates in the decomposition enthalpy of an ammonia salt, which is higher than the vaporization enthalpy of ammonia: $\Delta_r H^0 \approx 2.L_{vap}$): $\tau_w$ does not exceed 14 %.

Considering exergy efficiencies:

- The most performant cycle is the ORC ($\eta_{ex}$ ranges from 0.40 to 0.52) because it provides a full power output ($\tau_w = 100$ %, more exergy content than a cold output) with relatively low requirements in heat supply (the main part of $Q_{in}$ consists in a vaporization enthalpy, whereas it is a decomposition enthalpy for hybrid thermochemical cycles).
- Among hybrid thermochemical cycles, combined power & cold mode shows the best values in each of the three temperature areas: $\eta_{ex}$ ranges from 0.20 to 0.41. This is due to the fact that power production is maximized in comparison with separated and simultaneous modes. Concerning power mode with auto-thermal step, $\eta_{ex}$ increases with $T_{hot}$ (because power production increases with pressure $P_6$) and would probably exceed exergy performances of the combined mode if higher hot source temperatures than $T_{hot,max}$ were considered.

For all of the five systems, specific exergy output increases when $T_{hot}$ rises, which is directly related to the increase in expansion ratios. Moreover:

- Combined power & cold mode exhibits the highest values, over the whole range of hot source temperatures where it is feasible: $w+ex_{cold}$ ranges from 282 to 639 kJ/kg$_{NH3}$.
- For simultaneous power & cold mode, $w+ex_{cold}$ increases in the area [107; 195 °C], then remains almost constant between 440 and 485 kJ/kg$_{NH3}$. This is due to the fact that $P_{synth,H} = P_6$ reaches the boundary value $P_{min}$ when hot source temperature is around 195 °C, then remains constant so that expansion ratio does not increase anymore for $T_{hot} > 195$ °C.
- $w$ ranges from 90 to 162 kJ/kg$_{wf}$ for ORC, which is quite lower than the previous values. However, since ORC does not provide cold, a fair comparison should be done using (9) to compute the mass density of mechanical work in the case of cogeneration cycles.
- Finally, power mode with auto-thermal step shows quite good specific exergy outputs:
  - It reaches 596 kJ/kg$_{NH3}$ in resorption case. Since resorption cycle uses a solid reactive salt instead of ammonia as the LTM, no additional cold production may be provided at the outlet of the expander ($T_9$ is not low enough on Fig. 2), thus $\tau_w = 100$ %.

- $w+ex_{cold}$ ranges between 40 and 575 kJ/kg$_{NH3}$ in single sorption case. This configuration is characterized by lower temperatures $T_5$, $T_6$ and $T_m$ than in resorption case: therefore, an additional cold production is provided at the expander outlet ($\tau_w$ ranges from 58 to 87 %).

Finally, the most performant systems are retrieved for each temperature area on Fig. 3:

- As regards energy efficiency, combined power & cold mode exhibits the best performance in areas [100; 150 °C] ($\eta_I = 0.51$) and [150; 200 °C] ($\eta_I = 0.51$), but is overcome in area [200; 250 °C] by the separated power & cold mode in resorption case ($\eta_I = 0.61$).
- ORC presents the highest exergy efficiencies in both of the three areas (with maximal values of $\eta_{ex} = 0.52$, 0.50 and 0.46 respectively).
- The highest specific exergy output is reached by combined power & cold mode in each of the three areas ($w+ex_{cold} = 325$ kJ/kg$_{NH3}$, 543 kJ/kg$_{NH3}$ and 640 kJ/kg$_{NH3}$ respectively).

However, the high values obtained for $\eta_I$ and $w+ex_{cold}$ in cogeneration modes should be moderated because of the relatively low values of $\tau_w$.

# 5. Conclusion

In addition to the discussions of §4. on performances, a key factor in choosing the most adequate system for a given application is **complexity**. ORC are typically easier to implement than thermochemical cycles: indeed, chemical sorption processes imply heat and / or mass transfer limitations. However, this increase in complexity comes with an interesting **storage feature**.
Using an innovative methodology to evaluate performances for a large variety of reactive salts, it was shown that hybrid thermochemical cycles can be of great interest to recover low grade heat from a hot source under 250 °C while providing an intrinsic energy storage feature:

- If a cold storage and production function is primarily needed, with low power requirements, separated power & cold mode is the most interesting option.
- If a power & cold storage and cogeneration function is desired, combined power & cold mode is the most performant system; however, although slightly less performant, simultaneous mode requires only one expansion device and can operate at lower hot source temperatures.
- If only power output is desired, ORC is a relevant option, reaching high exergy efficiencies; however, it provides no storage function, contrary to the power mode with auto-thermal step.

The range of energy efficiencies is [0.01; 0.61] for the proposed hybrid thermochemical cycles (with much higher values for cogeneration modes), against [0.08; 0.18] for ORC. Their range of exergy efficiencies is [0.01; 0.41] (highly depending on hot source temperature and mode), below that of ORC: [0.40; 0.52]. Finally, exergy densities increase with hot source temperature and reach particularly high values for the innovative hybrid cycles (640 kJ/kg$_{NH3}$, against 162 kJ/kg$_{wf}$ for ORC).

Fig. 4 summarizes the strengths and weaknesses of each studied cycle. It offers a tool for choosing the most adequate system to recover low grade heat from a given source, according to the needs.

Weak performances | Average performances | Good performances

| Characteristics : | Hybrid thermochemical cycles | | | | | | ORC |
|---|---|---|---|---|---|---|---|
| | **Separated** power & cold mode | | **Simultaneous** power & cold mode | **Combined** power & cold mode | Power mode with **auto-thermal** step | | |
| | Resorption cycle | Single sorption cycle | | | Resorption cycle | Single sorption cycle | |
| Valorization of low-grade waste heat | $T_{hot} > 212$ °C | $T_{hot} > 138$ °C | $T_{hot} > 107$ °C | $T_{hot} > 138$ °C | $T_{hot} > 130$ °C | $T_{hot} > 81$ °C | *Wider range* |
| Power production | $\tau_w < 12.5$ % | $\tau_w < 14.3$ % | $\tau_w < 25.5$ % | $\tau_w < 30.1$ % | $\tau_w = 100$ % | $\tau_w > 57.6$ % | $\tau_w = 100$ % |
| Storage of the power production | | | | | | | |
| Cold production | | | | | | | |
| Storage of the cold production | | | | | | | |
| Specific exergy output (**kJ/kg$_{wf}$**) | $w + ex_{cold} < 448$ | $w + ex_{cold} < 273$ | $w + ex_{cold} < 485$ | $w + ex_{cold} < 640$ | $w + ex_{cold} < 575$ | $w + ex_{cold} < 596$ | $w + ex_{cold} < 162$ |

*Figure 4. Summary of the advantages and weaknesses of the five systems.*

## Acknowledgments

Alexis Godefroy receives a PhD grant from the Ministry of Education (doctoral contract n° 2017-09-ED.305).

## Nomenclature

| | |
|---|---|
| $\dot{m}$ | mass flow rate, kg/s |
| ex | mass density of exergy, J/kg |
| Ex | exergy, J |
| H | enthalpy, J |
| L | molar latent heat, J/mol |
| m | mass, kg |
| P | pressure, bar |
| q | mass density of heat, J/kg |
| Q | amount of heat, J |
| R | constant of the ideal gas law, J/(mol.K) |
| $R_v$ | volumetric expansion ratio, - |
| S | entropy, J/K |
| $\mathcal{S}$ | molar entropy, J/(mol.K) |
| T | temperature, °C |
| v | specific volume, $m^3/kg$ |
| w | mass density of mechanical work, J/kg |
| W | mechanical work, J |
| x | vapour quality, - |

### Greek symbols

| | |
|---|---|
| η | efficiency |
| τ | ratio |
| Δ | gap |
| $\Delta_r$ | Lewis operator (chemical reaction) |

### Subscripts and superscripts

| | |
|---|---|
| 0 | reference state |
| I | energy-related ($1^{st}$ principle) |
| amb | ambient temperature level |
| cold | cold temperature level |
| cond | condensation |
| dec | decomposition reaction |
| evap | evaporation |
| ex | exergy-related ($2^{nd}$ principle) |
| hot | hot temperature level |
| H | high temperature salt |
| HX1 | liquid/vapour or liquid/liquid heat exchange |
| HX2 | vapour/vapour heat exchange |
| in | input |
| is | isentropic |

| | |
|---|---|
| L | low temperature salt |
| m | medium temperature level |
| max | maximal value |
| min | minimal value |
| r-eq | chemical reaction equilibrium |
| synth | synthesis reaction |
| v | volumetric |
| vap | vaporization |
| w | mechanical work |
| wf | working fluid |

## References


[1] Aydin D., Casey S., Riffat S., The latest advancements on thermochemical heat storage systems, Renewable and Sustainable Energy Reviews 2015;41:367-356.

[2] Cabeza L. F., Solé A., Barreneche C., Review on sorption materials and technologies for heat pumps and thermal energy storage, Renewable Energy 2017;110:39-3.

[3] Kalina A., Combined cycle and waste heat recovery power systems based on a novel thermodynamic energy cycle utilizing low-temperature heat for power generation. ASME Joint Power Generation Conference; 1983 Sep 25-29; Indianapolis, USA.

[4] Xu F., Goswami D., Bhagwat S., A combined power / cooling cycle, Energy 2000;25:246-233.

[5] Hasan A., Goswami D., Vijayaraghavan S., First and second law analysis of a new power and refrigeration thermodynamic cycle using a solar heat source, Solar Energy 2002;73(5):393-385.

[6] Karimi M., Dutta A., Kaushik A., Bansal H., Haqu S., A review of Organic Rankine, Kalina and Goswami cycle, Int. Journal of Eng. Technology, Management and App. Sciences 2015;3.

[7] Jiang L., Lu Y., Roskilly A., Wang R., Wang L., Tang K., Exploration of ammonia resorption cycle for power generation by using novel composite sorbent, App. Energy 2018;215:467-457.

[8] Wang L., Ziegler F., Roskilly A., Wang R., Wang Y., A resorption cycle for the cogeneration of electricity and refrigeration, Applied Energy 2013;106:64-56.

[9] Lu Y., Wang Y., Bao H., Yuan Y., Wang L., Roskilly A., Analysis of an optimal resorption cogeneration using mass and heat recovery processes, Applied Energy 2015;160:901-892.

[10] Jiang L., Wang L., Zhang X., Liu C., Wang R., Performance prediction on a resorption cogeneration cycle for power and refrigeration with energy storage, Renewable Energy 2015;83;1259-1250.

[11] Jiang L., Wang L., Liu C., Wang R., Experimental study on a resorption system for power and refrigeration cogeneration, Energy 2016;97;190-182.

[12] Bao H., Wang Y., Roskilly A., Modelling of a chemisorption refrigeration and power cogeneration system, Applied Energy 2014;119:362-351.

[13] Stitou D., Mazet N., Mauran S., Experimental investigation of a solid/gas thermochemical storage process for solar air-conditioning, Energy 2012;41:270-261.

[14] Fitó J., Coronas A., Mauran S., Mazet N., Stitou D., Definition and performance simulations of a novel solar-driven hybrid absorption-thermochemical refrigeration system, Energy Conversion and Management 2018;175:312-298.

[15] F-Chart Software: Engineering Software EES: Engineering Equation Solver http://www.fchart.com/ees/.

[16] Touzain P., Thermodynamic values of ammonia salts reactions for chemical sorption heat pump. Proceedings of the International Sorption Heat Pump Conference; 1999 Mar 24-26; Munich, Germany.